Published in final edited form as:
Conf Proc IEEE Eng Med Biol Soc. 2012 ; 2012: . doi:10.1109/EMBC.2012.6346481.

Point Process Modeling Reveals Anatomical Non-Uniform Distribution across the Subthalamic Nucleus in Parkinson's Disease

Gilda Pedoto [Member, IEEE], **Sabato Santaniello [Member, IEEE]**, **Giovanni Fiengo [Member, IEEE]**, **Luigi Glielmo [Member, IEEE]**, **Mark Hallett**, **Ping Zhuang**, and **Sridevi V. Sarma [Member, IEEE]**

Abstract

Deep brain stimulation (DBS) is a highly promising therapy for Parkinson's disease (PD). However, most patients do not get full therapeutic benefit from DBS, due to its critical dependence on electrode location in the Subthalamic Nucleus (STN). For this reason, we believe that the development of a novel surgical tool for DBS placement, i.e., an automated intraoperative closed-loop DBS localization system, is essential. In this paper, we analyze single unit spiking activity of 120 neurons in different STN locations collected from 4 PD patients. Specifically, for each neuron, we estimate a point process model (PPM) of the spiking activity for different depths within the STN by which we are able to detect pathological bursting and oscillations. Our results suggest that these signatures are more prominent in the dorsolateral part of the STN. Therefore, accurately placing the DBS electrode in this target may result in maximal therapeutic benefit with less power effort required by DBS. Furthermore, PPMs might be an effective tool for modeling of the STN neuronal activities as a function of location within the STN, which may pave the way towards developing a closed-loop navigation tool for optimal DBS electrode placement.

I. Introduction

An estimated 6.5 million people have Parkinson's disease (PD), a movement disorder with a broad spectrum of symptoms, like predominant resting tremor, akinesia and rigidity [1]. Unfortunately, there is no treatment to stop disease progression. Deep Brain Stimulation (DBS) injects a current that alters the neural activity of the diseased brain circuit, which may lead to a reversal of PD symptoms. When appropriately stimulated, patients can regain control of movement and reduce medication use [2].

Although clinically accepted, DBS has side effects and the therapeutic effectiveness is often limited, because of its critically dependence on the location of the stimulating electrode and the relative distance of such a location from the "sweet spot", i.e., a motor-related region within the dorsal, lateral posterior portion of the subthalamic nucleus (STN) [3][4]. DBS in the sweet spot has been reported to be highly effective [5], with 60–70% of the implanted patients improving so markedly that medications are no longer required. The intra-operative localization and access to the sweet spot, however, remains a challenge as there is no consistent protocol used by neurosurgeons to reach this target accurately.

In order to quantitatively identify this target region, a framework for neural modeling, estimation and control of the STN is needed. This framework should be different from existing navigation tools, which guide the neurosurgeon from the cortex to the STN [6][7]. Such a navigation system (Fig. 1) consists of: (a) a predictive model that characterizes how the spike trains (output of G) of the neurons are generated as a function of STN or electrode position (neural system G); (b) an estimator that processes the spike trains from G to

estimate the electrode's distance from the sweet spot (a priori characterized for each patient through imaging); (c) a feedback controller, that accounts for the electrode's navigation dynamics and "steers" the electrode (i.e., actuates the electrode) to move closer to the sweet spot, based on the distance estimated in (b).

In this paper, we develop preliminary models of STN activity from spike train data collected from 120 STN neurons in 4 PD patients. We construct point process models (PPMs) for each neuron and analyze the PPM model parameters at several depths within the stimulation target [9][10]. Our results indicate that the incidence of bursting activity and pathological beta band oscillations are predominant in the dorsolateral part of the STN. This would suggest a depth-varying model for G, in which the instantaneous firing rate of the neurons changes as a function of the depth.

II. Methods

A. Human Data

Four patients undergoing DBS for the treatment of PD were included in the study. All patients had idiopathic PD with a Hoehn-Yahr score [8] of 3 or higher and had a documented response to L-dopa replacement therapy. All patients received a thorough pre-operative neurological exam. Patients had no cognitive impairment, active psychiatric disorders, or anatomic abnormalities on magnetic resonance imaging (MRI) [10], and none of the patients had undergone prior surgery for the treatment of PD. Informed consent for the study was obtained in strict accordance with a protocol approved by the Institutional Review Board at the Xuanwu Hospital.

B. Electrophysiology

Anti-PD medications were withheld the night before surgery. No sedatives were given prior to or during performance of recordings [11]. Single-unit recordings were made from the top to the bottom of the dorsal-lateral motor sub-territory of the STN based on stereotactic localization and reconstructions of the electrode trajectories [4]. Recordings were made at different depths along the trajectory targeting to the STN in .5mm increments, starting from 15 mm of depth (dorsal border), and going up to 28.5 mm (ventral border).

We used an array of 3 tungsten microelectrodes, separated by 2 mm and placed in a parasagittal orientation. Neuronal activity was band-pass filtered (300 Hz – 6 kHz) and sampled at 12 kHz. Spikes were detected by using the continuous wavelet transform algorithm [12]. The spike sorting was performed with WaveClus [13]. A total of 120 neurons across the four patients were classified by the neurophysiologist involved in the study as belonging to the STN.

C. Point Process Modeling of STN Dynamics

We formulate a point process model [8][14] to relate the spiking propensity of each STN neuron to factors associated with the depth of the STN recorded data as well as intrinsic factors such as the neuron's own spiking history. A point process is a series of 0–1 random events that occur in continuous time. It's the model of a neural spike train and it can be completely characterized by its conditional intensity function (*CIF*), $\lambda(t \mid H_t)$, defined as

$$\lambda(t|H_t) \equiv \lim_{\Delta \to 0} \frac{\Pr((N(t+\Delta t) - N(t)=1)|H_t)}{\Delta} \quad (1)$$

where H_t denotes the history of spikes up to time t. It follows from (1) that the probability of a single spike in a small interval $(t, t+\Delta]$ is approximately

$$\Pr(spike\ in(t, t+\Delta]|H_t) \cong \lambda(t|H_t)\Delta. \quad (2)$$

Details can be found [8][14]–[17]. When Δ is small, (2) is approximately the spiking propensity at time t.

The CIF generalizes the rate function of a Poisson process to a rate function that is history dependent. Because the conditional intensity function completely characterizes a spike train, defining a model for the CIF defines a model for the spike train [13][15]. For our analyses, we use generalized linear models (GLM) [16] to fit each CIF estimate framework for conducting statistical inferences [17].

Specifically, for each STN neuron the CIF is modeled as a function of (i) the neuron own spike history, and (ii) the spiking history of any other neuron simultaneously recorded For each neuron, the CIF has a multiplicative structure [18]:

$$\lambda(t|H_t, \Theta)=e^{\alpha t} \cdot \lambda^0(t|H_t^0, \beta) \quad (3)$$

where α is a constant history-independent term, $\lambda^0(t|H_t^0, \beta)$ describes the effect of the neuron's own spike history (H_t^0) on the neural response, $\Theta \equiv [\alpha, \beta]$ is a parameter vector to be estimated from data. $\lambda^0(t|H_t^0, \beta)$ is dimensionless. The CIF model (3) typically has a multiplicative structure: it is composed of distinct CIFs for each different kind of covariates, in order to assess how much each component contributes to the spiking propensity of the neuron. In this work, we choose to estimate the intensity as function of the neuron's own history. If the spiking history is not a significant factor associated with the neural response, then $\lambda^0(t|H_t^0, \beta)$ will be very close to 1 for all time and (3) reduces to an inhomogeneous Poisson process. The CIF is as follows:

$$\lambda^0(t|H_t^0, \beta) = \exp\left\{\sum_{r=1}^{10}\beta_r N(t-r+1:t-r)+\sum_{l=1}^{20}\beta_{10+l}N(t-10-2l:t-10-2(l-1))+\sum_{j=1}^{15}\beta_{30+j}N(t-50-10j:t-50-10(j-1)\right. \quad (4)$$

with $\beta=\{\beta_i\}_{i=1}^{55}$ and $N(a:b)$ being the number of spikes observed in the time interval $[a, b)$. Parameters $\{\beta_i\}_{i=1}^{10}$ measure the effects of the spiking history in the previous 10 ms and therefore can capture refractoriness and/or bursting on the spiking probability. Parameters $\{\beta_i\}_{i=11}^{30}$ and $\{\beta_i\}_{i=31}^{45}$ instead, measure respectively the effect of the spike history from 10 to 50 ms (with 2 ms-long bins) and from 50 to 200 ms (with 10 ms-long bins) prior the time t, and can capture oscillations in the beta frequency band (13–35 Hz). Parameters $\{\beta_i\}_{i=46}^{55}$ measure the effect of the spiking history from 200 to 500 ms (with 30 ms-long bins) prior the time t, and can capture oscillations in the tremor band (3–6 Hz).

Because of its optimality properties, we choose a likelihood approach for fitting and analyzing the parametric model of the conditional intensity function. Parameters are efficiently computed using the iterative reweighted least squares algorithm. Goodness of fit was measured by applying the time-rescaling theorem for point process models and computing the Kolmogorov-Smirnov statistic (Johnson and Kotz, 1970).

D. Point Process Analysis

Once a point process model was estimated for each neuron at each recording depth, we determined whether the neuron's spike train exhibited *(i)* prominent short term excitatory patterns (e.g. period <10 ms, corresponding to intra-burst activity), *(ii)* oscillations in the 15–33 Hz beta frequency band, and *(iii)* oscillations in 3–6 Hz tremor band. We assessed these signatures directly from the model parameters and their 95% confidence bounds. Specifically, a neuron has an excitatory pattern if one or more of the history parameters $\{\beta_i\}$corresponding to bins in ms in the past satisfies the **excitatory pattern condition**: for at least one i in the time range, $LB_i \geq 1$ and $UB \geq 1.5$, where $LB_i \leq e^{\beta i} \leq UB_i$, and LB_i and UB_i are the 95% lower and upper confidence bounds of β_i, respectively. In the following, typical signatures captured by our model:

- ***Short-term excitatory pattern:*** a neuron exhibits a short term pattern if the model parameters $\{\beta_i\}_{i=2}^{10}$ satisfy the excitatory pattern condition (Fig. 3, yellow oval).
- ***15–33 Hz Oscillations:*** a neuron exhibits a (non)-stationary oscillation with frequency between 15 and 33 Hz if the model parameters $\{\beta_i\}_{i=20}^{32}$ satisfy the excitatory pattern condition (Fig. 3, blue oval).
- ***3–6 Hz Oscillations:*** a neuron exhibits a (non)-stationary oscillation with frequency between 3–6 Hz, if the model parameters $\{\beta_i\}_{i=41}^{50}$ satisfy the excitatory pattern condition (example not shown).

III. Results

120 neurons were recorded and sorted from the STN across the four patients at several depths within the nucleus. Since the STN has different dimensions in each patient (its length ranges from 3.5mm to 6.5 mm) [3], we normalize recording depths, by indicating with 0 the dorsal border of the nucleus, and with −1 the ventral border, stepping in increments of −0.1 (Fig. 2). Neurons were grouped on the basis of the recording depths, in order to allow the analysis of how many neurons exhibit pathological oscillations going into the stimulation target. A point process model was computed for each sorted neuron and model parameters were analyzed.

A. Dorsoventral Patterns within STN

The analysis of model parameters was performed, as indicated in section II.D, and we summarized results in the histograms of Fig. 4. If we look at the depth range [0,−0.5], corresponding to the dorso-lateral region of the STN (red rectangular in Fig.4), a larger number of neurons exhibit signatures compared to the ventral part. The analysis, in fact, shows that there is a prevalence to short-term/bursting pattern and pathological oscillations, both in the tremor and β-band. These results suggest that bursting pattern, that have been studied for a long time in the STN and other basal ganglia (i.e. [21]–[25]), are not uniformly distributed, and confirm the hypothesis that β-oscillatory activity is seen largely within the dorsolateral portion of the STN [4], the same location that seems to provide optimal therapeutic benefit to patient undergoing STN DBS. Therefore, the predominance of tremor and β-band oscillations detected in the dorsal STN, confirms the spatial pattern of neuronal oscillatory frequency distribution within the STN [1][3]. Our point process models appear to predict the spiking activity of a neuron at each STN depth.

B. Towards a Mean Model: parameters' analysis

For each depth range, we computed the mean parameters vvector across all recorded neurons, In this way, we have a mean model for each depth range, and in Fig. 5. A

parameters of this model are plotted as a function of depth. We observe that values of β_{mean} become more intense (yellow-red areas) for depths in [0,−.5] in correspondence of *1–10 ms*, *35–74 ms* and *166–333 ms* time bins. The mean model confirms the predominance of bursting, β and tremor oscillations in the dorsal portion of the STN.

C. Statistical Test

Fig. 4 indicated that neurons exhibiting burst activity and significant oscillations are localized significantly more in the first half of the STN than in the second one (χ^2 test, $p< 0.05$). Furthermore, we partitioned the STN into three consecutive regions and found that neurons in the first 1/3 had PPM parameters significantly different from those in the remaining two regions (ANOVA test, $p<0.05$).

IV. Conclusions

On a preliminary dataset of 120 STN neurons recorded in four PD subjects undergoing DBS electrode placement surgery, we found that there our PPMs were able to capture short term patterns, often identified with bursting activity and pathological oscillations both in tremor and β-frequency range. Overall, these results were not uniformly distributed, across the STN volume but mostly localized in the dorsolateral portion of the STN, thus suggesting the existence of a sweet spot where the pathological features related to the PD are likely concentrated. Furthermore, the analysis of the PPM parameter values indicate that the signature features of PD in the STN neurons can be modeled as a function of the location, suggesting that a model for the system G in Fig.1 can be viable.

Acknowledgments

Support to S.V.S is provided by Burroughs Wellcome Fund CASI Award 1007274; National Science Foundation CAREER Award 1055560; NIH R01NS073118-02.

References

1. Tass P, Smirnow D, Karavaev A, Barnikol U, Barnikol T, Adamchic I, Hauptmann C, Pawelcyzk N, Maarouf M, Sturm V, Freund HJ, Bezruchko B. The causal relationship between subcortical local field potentials oscillations and Parkinsonian resting tremor. Journal of neural Engineering. 2010 Jan.vol.7:16. 016009.
2. Bergman, H.; Wichmann, T.; DeLong, MR. Reversal of experimental parkinsonism by lesions Book Series Mathematics in Industry. Vol. vol. 8. Berlin: Springer Heidelberg; 1990. 1990.
3. Contarino MF, Bour LJ, Bot M, van den Munckhof P, Speelman JD, Schuurman PR, de Bie RM. Tremor-specific neuronal oscillation pattern in dorsal subthalamic nucleus of parkinsonian patients. Brain Stimulation. 2011 Mar. Article in Press.
4. Weinberger M, Hutchison WD, Lozano AM, Hodaie M, Dostrovsky JO. Increased gamma oscillatory activity in the subthalamic nucleus during tremor in Parkinson's disease patients. J. Neurophysiol. 2009 Feb.vol. 101:789–802. [PubMed: 19004998]
5. Johansson JD, Blomstedt P, Haj-Hosseini N, Bergenheim AT, Eriksson O, Wådell K. Combined Diffuse Light Reflectance and Electrical Impedance Measurements as a Navigation Aid in Deep Brain Surgery. Stereotact Funct Neurosurg. 2009 Feb.vol.87:105–113. [PubMed: 19223697]
6. Wong S, Baltuch GH, Jaggi JL, Danish SF. Functional localization and visualization of the subthalamic nucleus from microelectrode recordings acquired during DBS surgery with unsupervised machine learning. J. Neural Eng. 2009; vol. 6:11.
7. Snyder, DL.; Miller, MI. Random Point Processes in Time and Space. New York, NY: Springer; 1991.
8. Sarma SV, Eden UT, Cheng ML, Williams ZM, Eskandar E, Brown EN, Hu R. Using point process models to compare neural spiking activity in the subthalamic nucleus of Parkinson’s patients and a normal primate. IEEE Trans. Biomed. Eng. 2010 Jun.vol. 56:1297–1305. [PubMed: 20172804]

9. Goetz CG, Poewe W, Rascol O, Sampaio C, Stebbins GT, Counsell C, Giladi N, Holloway RG, Moore CG, Wenning GK, Yahr Melvin D, Seid L. Movement Disorder Society Task Force Report on the Hoehn and Yahr Staging Scale: Status and Recommendations. Movement Disorder. 2004 Sep; Vol. 19(No. 9):1020–1028.
10. Amirnovin R, Williams ZM, Cosgrove GR, Eskandar. Visually guided movements suppress subthalamic oscillations in Parkinson's disease patients. J. Neurosci. 2004; vol. 24(50):11302–11306. [PubMed: 15601936]
11. Hutchison WD, Allan RJ, Opitz H, Levy R, Destrovsky JO, Lang AE, Lozano AM. Neurophysiological identification of the subthalamic nucleus in surgery in parkinson's disease. Ann. Neurol. 1998 Oct.vol. 4:622–628. [PubMed: 9778260]
12. Nenadic Z, Burdick JW. Spike Detection using the continuous wavelet transform. IEEE TBE. 2005 Jan; vol. 52(1):74–87.
13. Quian Quiroga R, Nadasdy Z, Ben-Shaul Y. Unsupervised Spike detection and sorting with wavelets and superparamagnetic clustering. Neural Comp. 2004 Aug.vol. 16(no. 8):1661.
14. Eden UT, Amirnovin R, Brown EN, Eskandar EN. Constructing Models of the Spiking Activity of Neurons in the Subthalamic Nucleus of Parkinson's Patients. Joint Statistical Meetings (JSM). 2007
15. Truccolo W, Eden UT, Fellow MR, Donoghue JP, Brown EN. A point process framework for relating neuronal spiking activity for spiking history, neural ensemble and extrinsic covariate effects. J Neurophys. 2005; vol. 93:1074–1089.
16. Brown, EN. Theory of Point Processes for Neural Systems. In: Chow, CC.; Gutkin, B.; Hansel, D.; Meunier, C.; Dalibard, J., editors. Methods and Models in Neurophysics. Vol. Ch. 14. Paris: Elsevier; 2005. p. 691-726.
17. Brown, EN.; Barbieri, R.; Eden, UT.; Frank, LM. Likelihood methods for neural data analysis. In: Feng, J., editor. Computational Neuroscience: A Comprehensive Approach. Vol. Chapter 9. London: CRC; p. 253-286.
18. McCullagh, P.; Nelder, JA. Generalized linear models. 2nd ed.. Boca Raton, FL: CRC; 1990.
19. Kass RE, Ventura V. A spike-train probability model. Neural Comput. 2001 Aug.vol.13:1713–1720. [PubMed: 11506667]
20. Hahn PJ, McIntyre CC. Modeling shifts in the rate and pattern of subthalamopallidal network activity during deep brain stimulation. J Comp Neurosci. 2010 Jun.vol. 28:425–441.
21. Brown P, Williams PD. Basal ganglia local field potential activity: character and functional significance in the human. Clinical Neurophysiology. 2005 Nov.vol. 116:2510–2519. [PubMed: 16029963]
22. Goldberg JA, Kats SS, Jaeger D. Globus pallidus discharge is coincident with striatal activity during global slow wave activity in the rat. Journal of Neuroscience. 2003; vol. 23:10058–10063. [PubMed: 14602820]
23. Goldberg JA, Rokni U, Boraud T, Vaadia E, Bergman H. Spike synchronization in the cortex/basal-ganglia networks of Parkinsonian primates reflects global dynamics of the local field potentials. Journal of Neuroscience. 2004 Jun.vol. 24:6003–6010. [PubMed: 15229247]
24. Pedoto, G.; Santaniello, S.; Montgomery, EB.; Gale, JT.; Fiengo, G.; Glielmo, L.; Sarma, SV. System Identification of local Field Potentials under Deep Brain Stimulation in a Healthy Primate. Proc. in 32nd Conference of the IEEE Engineering in Medicine and Biology Society; Aug.31st–Sept 4th, 2010; Buenos Aires.
25. Pedoto, G.; Santaniello, S.; Montgomery, EB.; Gale, JT.; Fiengo, G.; Glielmo, L.; Sarma, SV. Analyzing Local field Potentials in the Healthy basal ganglia under Deep Brain Stimulation. Proc. in 49th Conference on Decision and Control; Atlanta. Dec. 2010;

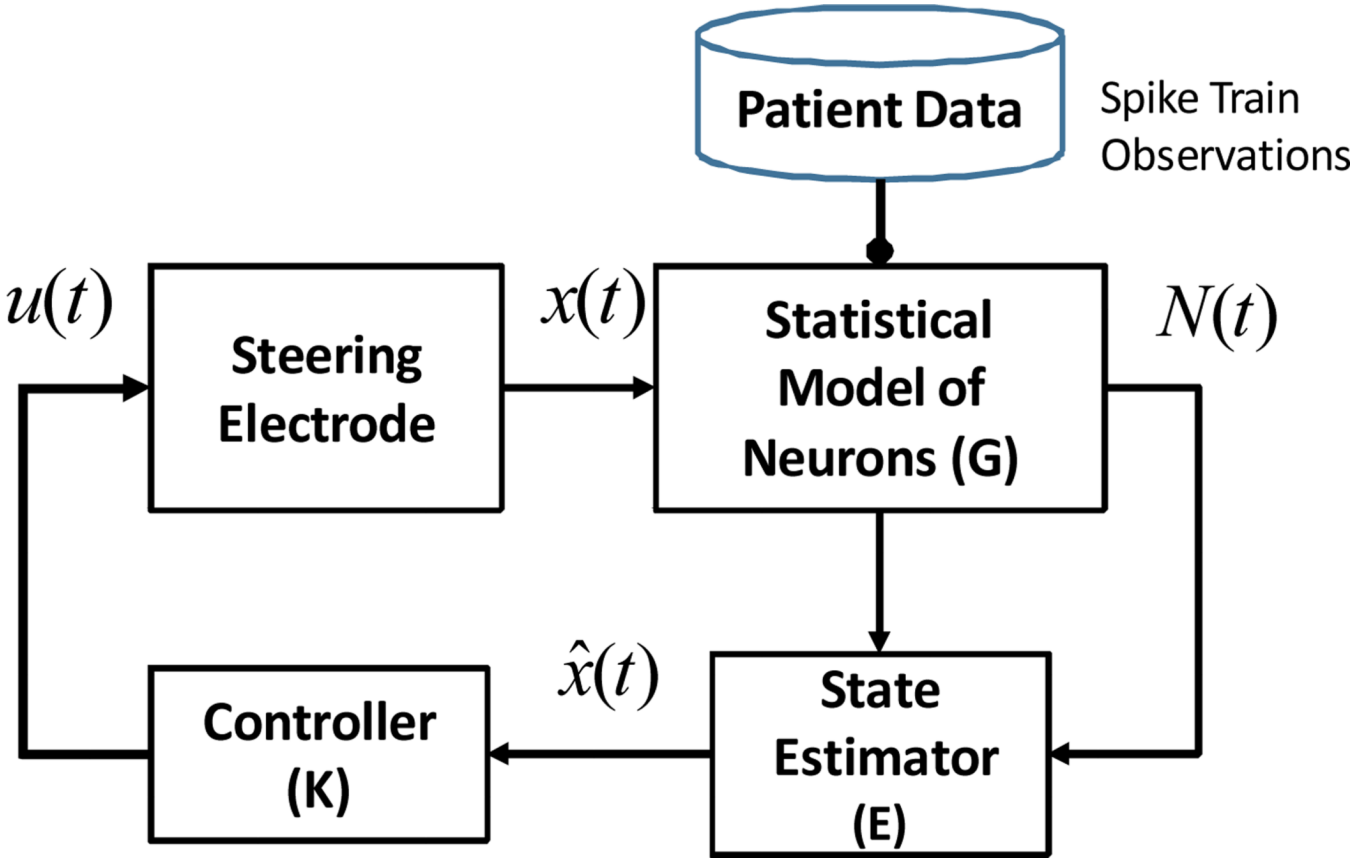

Fig. 1.
Schematic of DBS Navigation system.

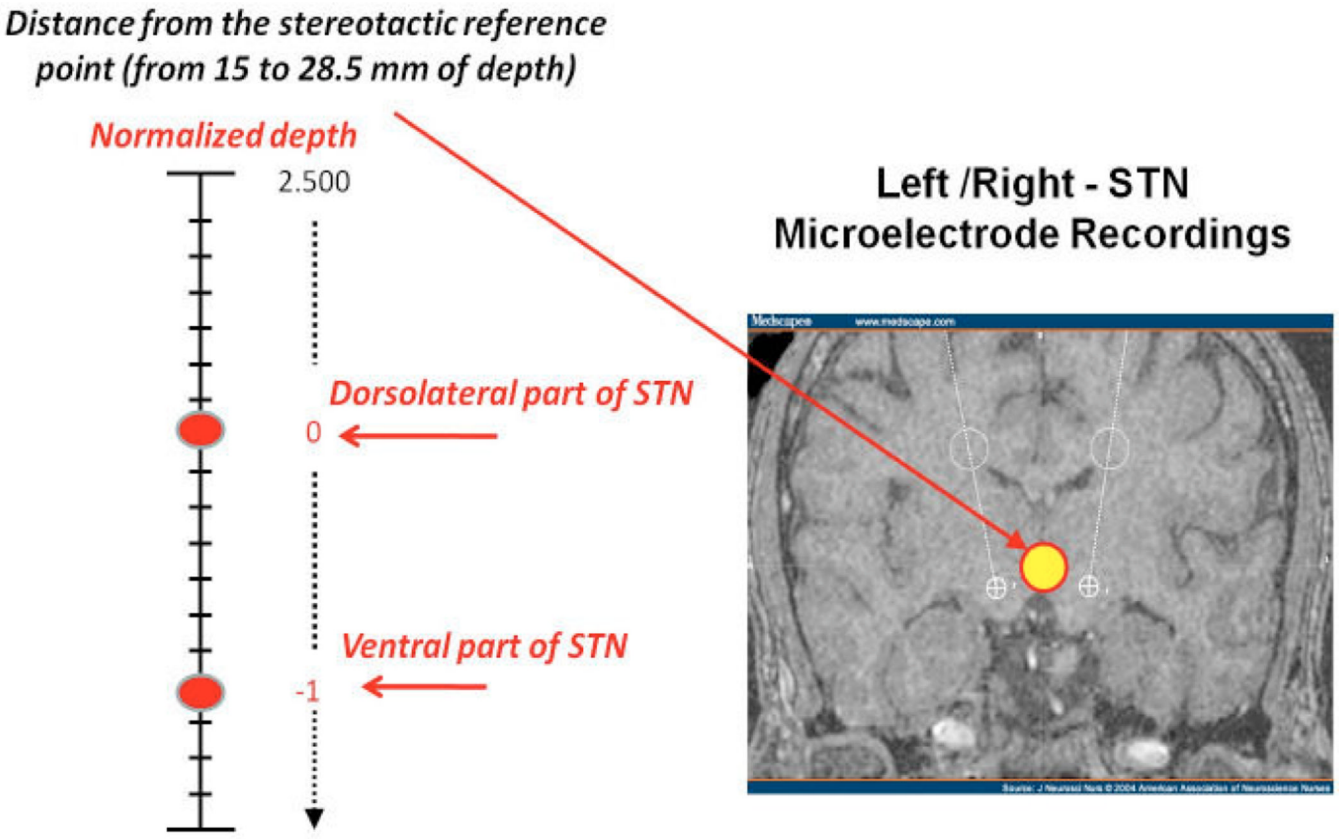

Fig. 2.
Recordings taken at different depths within the STN.

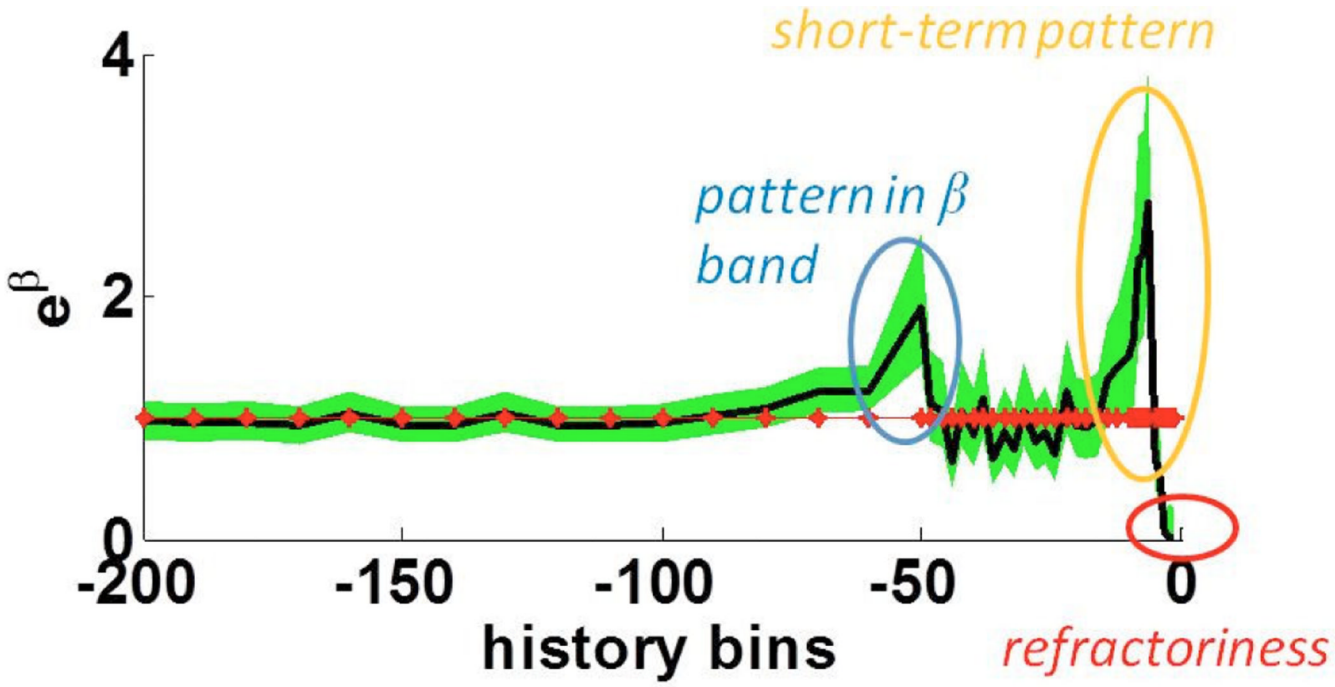

Fig. 3.
Point process model parameters β for a typical STN neuron and their confidence bounds for a single neuron. β measures the effects of spiking history on the spiking propensity of the modeled neuron.

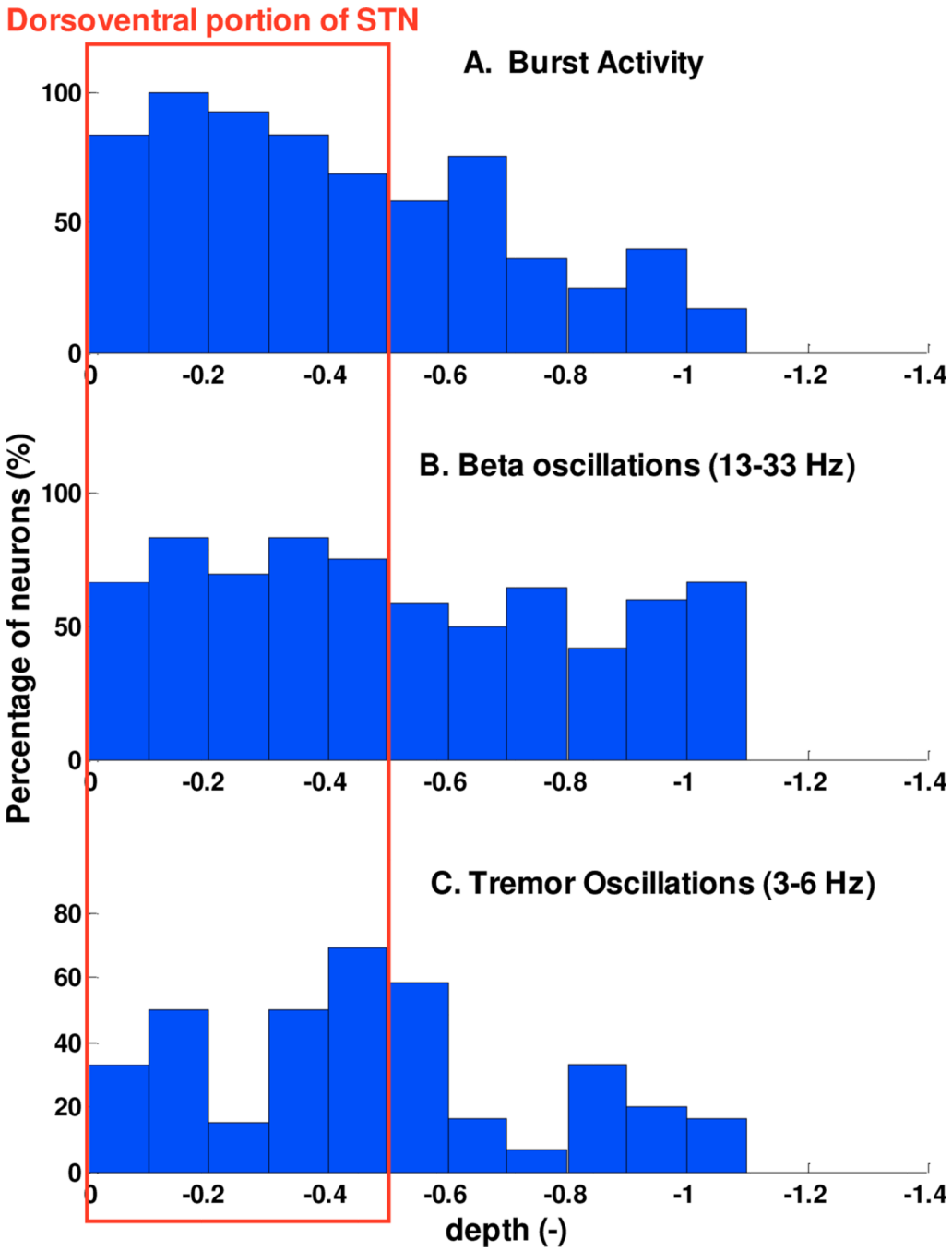

Fig. 4.
Histograms of percentage of neurons exhibiting signatures in function of depth: A) bursting, B) β oscillations and C) tremor-band oscillations.

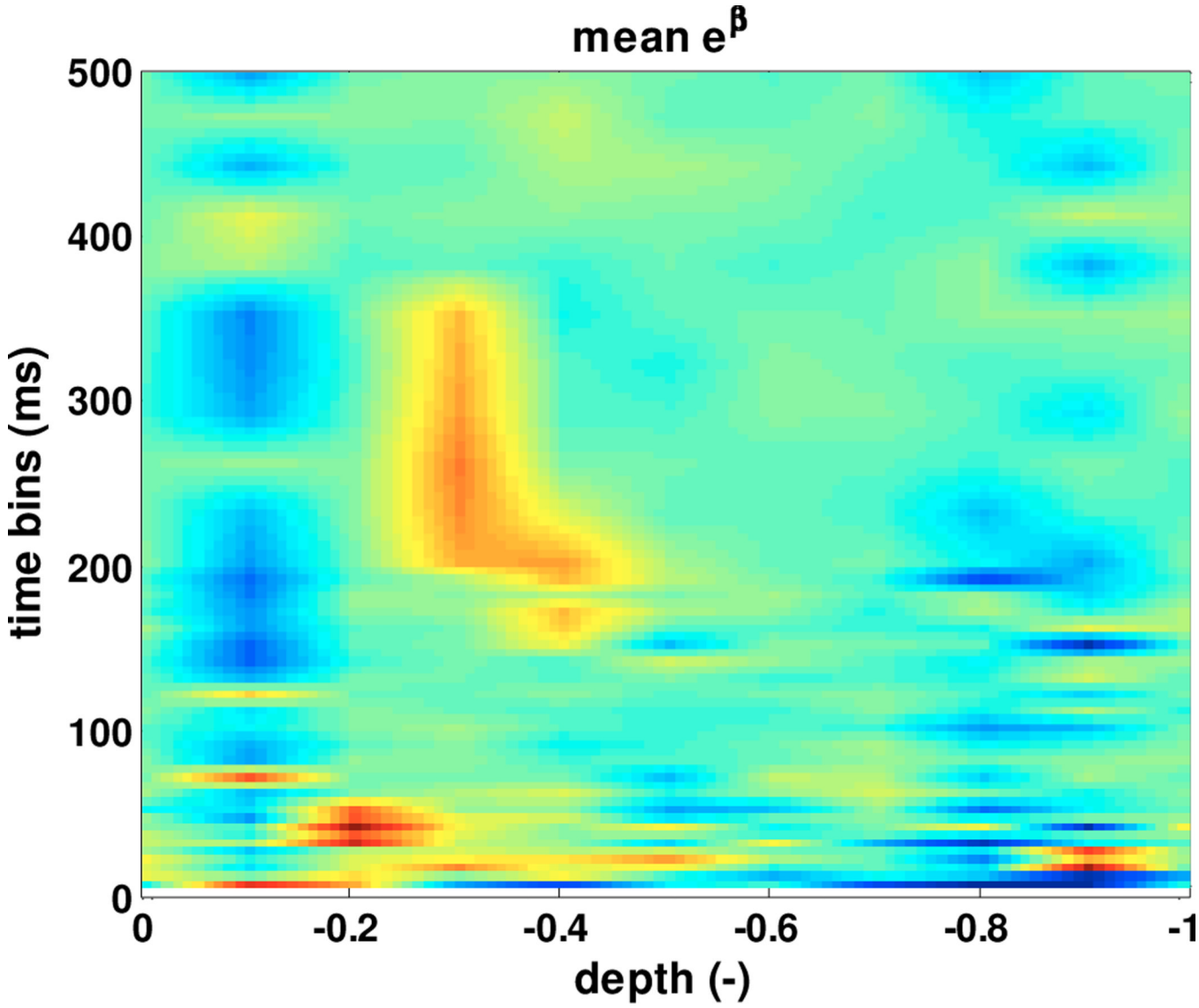

Fig. 5.
Mean model parameters.